

Design and development of test methodology for measuring hydrodynamic drag on fabric

Varshana Aruleswaran
Dept. of Textile and Apparel Engineering
University of Moratuwa
 Katubedda, Sri Lanka
 181048k@uom.lk

Thakshnavi Mahendran
Dept. of Textile and Apparel Engineering
University of Moratuwa
 Katubedda, Sri Lanka
 181047g@uom.lk

S N Niles
Dept. of Textile and Apparel Engineering
University of Moratuwa
 Katubedda, Sri Lanka
 nils@uom.lk

T S S Jayawardena
Dept. of Textile and Apparel Engineering
University of Moratuwa
 Katubedda, Sri Lanka
 jaya@uom.lk

Gayani K Nandasiri
Dept. of Textile and Apparel Engineering
University of Moratuwa
 Katubedda, Sri Lanka
 gayanin@uom.lk

Keywords—*hydrodynamic drag, fabric drag, CFD simulation, passive towing, mannequin shape.*

I. INTRODUCTION

Swimming is an intense sport demanding strength, endurance, and technical proficiency, necessitates maximizing performance advantages. Usually, optimized swimwear reduces drag for the swimmers. To continually enhance swimwear performance, manufacturers invest in innovative materials and techniques. However, still the swimwear efficiency is debated among industry experts. The past research studies have consistently demonstrated that swimmers allocate over 90% of their effort to counteract hydrodynamic resistance, underscoring the critical importance of swimwear design in optimizing speed and achieving successful outcomes [1]. Drag force is the resistance that a fluid puts up against an object as it moves in the opposite direction, slowing down the motion [2]. Any object moving through a fluid at a relative velocity will experience the drag. Fluid dynamic drag force can be mathematically expressed as

$$F_D = \frac{1}{2} \rho A U^2 C_D$$

where ρ is the fluid density, A is the reference area, U is the relative speed with reference to fluid and C_D is the drag coefficient [2].

II. LITERATURE REVIEW

Swimwear manufacturers strive to differentiate themselves by creating fabrics that minimize resistance. However, existing drag measurement techniques have limitations, such as measurement errors, subjective outcomes, and costly setups.

Drag measurement techniques are categorized as:

A. Passive towing

Allow direct drag measurement at a constant speed [3]. It assesses performance variables, energy expenditure, and drag forces [4], [5] and evaluates fabric drag [2], [4] and hydrodynamic properties. However, it differs from dynamic aquatic settings [6]. Hence holistic approach integrating passive towing with other methods enhances the measurement of hydrodynamic drag.

B. Inverse Dynamics

In swimming, a glide refers to the phase where a swimmer moves through the water without active propulsion. The push off glider method measures the hydrodynamic drag during this phase by analyzing velocity, deceleration, and resistive force. It simulates a swimmer's start or turn,

considering passive resistance [3]. However, this method has limitations in open water applicability and the specialized equipment requirements.

C. Prosthesis simulation method

Limb movements were simulated and drag was measured using a sensor attached to the limb. Poyhonen et al. [7] employed this method to investigate water exercise programs and prosthetic design. It enables controlled assessment of hydrodynamic drag, offering insights into body positions, limb movements, and the effect of equipment. However, limitations arise regarding real-life applicability, specialized equipment requirements, and constraints on sample size and data complexity.

D. Measure Active Drag (MAD) System

Measures the swimmer's active drag, correlating with mechanical power and swimming velocity [8]. However, the efficacy and individual variations that occurs in this method is questioned in existing literature[6]. Furthermore, drag value is usually represented as a mean value, however in reality, it fluctuates over time for swimmers, making a single mean value insufficient to represent real drag [9]. Despite considerations, it provides dynamic insights, requiring specialized equipment [6].

E. Computational Fluid Dynamics (CFD)

A versatile computational method widely utilized in aerospace, automotive, and marine engineering. It enables in depth analysis of fluid flow and drag, optimizing designs for improved performance and efficiency. Realistic boundary conditions and numerical models are employed to accurately simulate real-world scenarios and obtain meaningful results[10]. Thus, this study aims to recognize the limitations of inverse dynamics, prosthesis simulation, and the MAD system, including measurement errors, subjective results and to propose a test methodology to overcome these limitations. The study proposes a novel approach that combines computational fluid dynamics (CFD) analysis with passive towing, where this integration aims to address the limitations of CFD in replicating real-life scenarios and enhance the accuracy of passive towing outcomes by leveraging CFD analysis.

III. METHODOLOGY

Mannequin shape determination: This study selected a mannequin shape similar to the study conducted by Abasi et al.[2] with few adjustments accounting for the convenience of testing. While maintaining the general human body form, modifications were made to address challenges related to fabric wrapping on a curved figure.

The shape was modelled using AutoCAD 3D software, and surface area was calculated. However, drag is generated by the interaction between the fluid and a parallel surface, as well as the cohesive forces between fluid molecules [11] therefore effective surface area (A_{eff}) was determined by excluding leading and trailing surfaces.

The dimensions of the second mannequin, shaped like a cuboid, were adjusted to achieve a comparable effective frontal area (A_{eff}) as calculated for the figure shown in Fig. 3. Subsequently, the final shape of the mannequin was transformed into a cylindrical cylinder with a matching radius to ensure the same (A_{eff}) value.

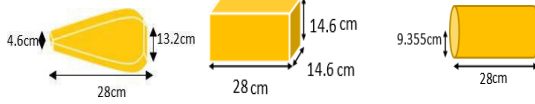


Fig. 1. Shape 1 Dimensions

Fig. 2. Shape 2 Dimensions

Fig. 3. Shape 3 Dimensions

CFD simulation: In ANSYS software, virtual mannequin models were created for drag effect simulations. Computational efficiency was improved by using half of the mannequin's geometry with symmetric boundary conditions. The simulation focused on the mannequin's surfaces within a cubic fluid flow region to assess drag effects.

A refined mesh accurately captured flow and determined drag forces around the mannequin. Boundaries were set to represent fluid behavior around fabric. The numerical simulation assumed an incompressible flow with a turbulence intensity of 10% and a turbulence scale of 0.10 m. The k-omega model was used to describe turbulent kinetic energy and its rate of dissipation.

ANSYS post-processing tools analyses results, visualizing fluid flow patterns and calculating drag forces on the mannequin.

Dimension analysis: The mannequin setup was scaled down by comparing it with the tank used in previous study in literature [2] ensuring compatibility with the new tank size.

Design of the test rig: The test rig was designed for the towing tank setup, including a mannequin stand, motor system for controlled towing and resetting, and a drag force measurement setup. Holes and a plastic tube reduced friction, while a securely mounted rig with a pulley ensured stability and alignment. A separate reset mechanism enabled automatic resetting, enhancing convenience, and minimizing manual handling.

Scale up the setup: To overcome the limitations of the benchtop equipment and enable a scale-up of the setup to a 15m pool with a width of 0.9m, modifications were made to accommodate the larger tank size. The adjustments included doubling the radius of the mannequin to match the pool width and implementing enhancements to the towing stand, trailing mechanism, tension adjustment, and tension measuring device. These modifications ensured precise tension control and improved guidance of the mannequin during towing. By modifying the existing towing stand with removable frames, the setup became versatile for both scaled-down and scaled-up experiments, promoting cost-effectiveness and practicality.

Material: Five commonly used fabric samples from the market were collected for testing. These fabric samples were subjected to testing at four different speeds, as detailed in Table 1.

TABLE I. SAMPLE DESCRIPTION

| The Sample code | The Sample | Fabric structure | Sample mass (g/cm ²) | Fiber composition (%) |
|-----------------|-----------------|---|----------------------------------|---------------------------|
| NM | Naked Mannequin | - | - | - |
| A | Fabric A | Stretch woven fabric | 130 | 75% nylon 25% elastane |
| B | Fabric B | Stretch woven fabric | 108 | 65% Nylon 35% Elastane |
| C | Fabric C | Single jersey circular knit | 245 | 77% Nylon 23% Lycra |
| D | Fabric D | Single jersey circular knit | 195 | 80% Nylon 20% Elastane |
| E | Fabric E | Single jersey circular knit (flock print) | 195 | 80% Nylon 20% Elastane |

IV. RESULT AND DISCUSSION

In this study, CFD simulation analyses pressure forces and velocity vectors on the mannequin, revealing different force patterns for various mannequin shapes.

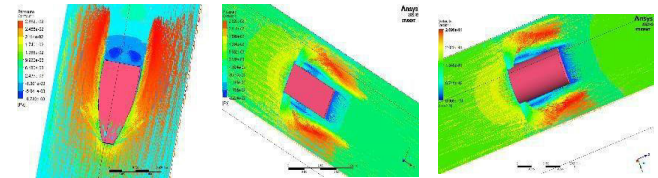


Fig. 4. Shape 1 contour

Fig. 5. Shape 2 contour

Fig. 6. Shape 3 contour

Fig.4. exhibits fewer scattered vectors on the front surface, intense vectors along the side, and visible turbulence on the back. Fig.5 and Fig. 6 with a larger frontal surface area, shows increased fluid interaction, scattering of vectors, and higher turbulence. Despite the smaller front surface area, shape1 experiences lower drag due to the presence of a boundary layer effect. The gradual increase in surface area towards the back creates a boundary layer that reduces turbulence and drag. Dense vectors observed around shape 1's side surfaces indicate smooth fluid flow, minimizing turbulence and drag.

To validate the analysis, drag force graphs were plotted for the mannequin walls, representing the drag force experienced by each shape. The graphs showed an initial peak followed by stability in the remaining iterations.

The experiment compared the drag performance of tubular fabric samples and bonded fabric samples. The results indicated that both types of fabric samples exhibited similar drag values at different testing speeds, suggesting that the bonding process did not significantly impact the drag performance. However, there were slight variations within the measured values, as indicated by the standard deviations.

Further analysis was conducted on three fabric samples (A, B, and C) and a naked mannequin (NM) at different speed levels. Fabric A showed the highest drag, while fabric

C exhibited the lowest drag in the initial speeds, but this pattern changed at high speed. To improve accuracy in future testing, recommendations were made, including using a different sensor with a higher sampling rate and increasing the tank dimensions to provide more space for the mannequin's movement.

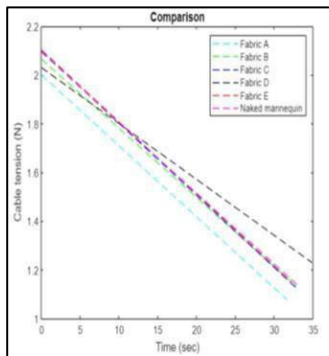


Fig. 7. Mean value comparison

The DHI strain gauge readings show fluctuations and decreasing trend in cable tension during underwater towing due to water currents, turbulent patterns, and cable dynamics. Drag cannot be simplified to a single value due to inherent variability throughout the swimming cycle, with mean values.

The comparison graph reveals the drag experienced by different fabrics and the naked mannequin. Fabrics A and B have the lowest GSM values, with Fabric A having higher nylon content contributing to its lower drag. Fabric B initially has lower cable tension but stretches during towing, matching the naked mannequin's tension. Fabric C's knitted structure enables it to conform closely, resulting in similar tension to the naked mannequin from the start. Fabric D exhibits high wettability, causing higher drag, while Fabric E's hydrophobic nature reduces drag. Surprisingly, the naked mannequin experiences higher cable tension than most fabric samples, challenging assumptions about drag solely influenced by weight. Surface properties of fabric samples play a significant role in drag force influence.

V. CONCLUSION

This research investigated on design and development of a testing methodology to measure hydrodynamic drag acting on a fabric, addressing the limitations of the existing measurement methods. By utilizing CFD analysis to determine the optimal mannequin shape the study emphasized the importance of selecting an optimal mannequin shape for accurate measurements. The results

showed that fabric A had higher drag due to its composition, texture, and weave construction, while fabric C exhibited the lowest drag due to its knit construction and smoother surface. The study also highlighted the limitations of benchtop equipment at high speeds due to space constraints. These findings contribute to a better understanding of fabric drag behavior and have implications for improving fabric design in various applications.

REFERENCES

- [1] H. Moria et al., "Contribution of swimsuits to swimmer's performance," in *Procedia Engineering*, Elsevier Ltd, 2010, pp. 2505–2510. doi: 10.1016/j.proeng.2010.04.023.
- [2] S. Abasi, T. Nasrollahi, M. Aghajani, and M. A. Tehran, "Construction of drag force measuring system to characterize the hydrodynamics properties of swimsuit fabrics," *Journal of Industrial Textiles*, vol. 43, no. 2, pp. 264–280, Oct. 2013, doi: 10.1177/1528083712452901.
- [3] A. P. Webb, D. J. Taunton, D. A. Hudson, A. I. J. Forrester, and S. R. Turnock, "Repeatable techniques for assessing changes in passive swimming resistance," *Proc Inst Mech Eng P J Sport Eng Technol*, vol. 229, no. 2, pp. 126–135, Jun. 2015, doi: 10.1177/1754337114562875.
- [4] P. Zamparo, G. Gatta, D. Pendergast, and C. Capelli, "Active and passive drag: The role of trunk incline," *Eur J Appl Physiol*, vol. 106, no. 2, pp. 195–205, 2009, doi: 10.1007/s00421-009-1007-8.
- [5] H. M. Toussaint et al., "Swimming: Effect of a fast-skin™ 'body' suit on drag during front crawl swimming," *Sports Biomech*, vol. 1, no. 1, pp. 1–10, Jan. 2002, doi: 10.1080/14763140208522783.
- [6] J. Buder and S. Odenwald, "Performance validation of swimsuits by mechanical testing," in *Procedia Engineering*, Elsevier Ltd, 2010, pp. 3373–3378. doi: 10.1016/j.proeng.2010.04.160.
- [7] T. Pöyhönen, K. L. Keskinen, A. Hautala, and E. Mälikä, "Determination of hydrodynamic drag forces and drag coefficients on human leg/foot model during knee exercise," *Clinical Biomechanics*, vol. 15, no. 4, pp. 256–260, May 2000, doi: 10.1016/S0268-0033(99)00070-4.
- [8] B. S. Roberts, K. S. Kamel, C. E. Hedrick, S. P. McLean, and R. L. Sharp, "Effect of a FastSkin™ suit on submaximal freestyle swimming," *Med Sci Sports Exerc*, vol. 35, no. 3, pp. 519–524, Mar. 2003, doi: 10.1249/01.MSS.0000053699.91683.CD.
- [9] A. Alcock and B. Mason, "Biomechanical analysis of active drag in swimming".
- [10] M. Bilinauskaite, V. R. Mantha, A. I. Rouboa, P. Ziliukas, and A. J. Silva, "Computational fluid dynamics study of swimmer's hand velocity, orientation, and shape: Contributions to hydrodynamics," *Biomed Res Int*, vol. 2013, 2013, doi: 10.1155/2013/140487.
- [11] B. Dean and B. Bhushan, "Shark-skin surfaces for fluid-drag reduction in turbulent flow: A review," *Philosophical Transactions of the Royal Society A: Mathematical, Physical and Engineering Sciences*, vol. 368, no. 1929. Royal Society, pp. 4775–4806, Oct. 28, 2010. doi: 10.1098/rsta.2010.0201.